ROBOMECH Journal

RESEARCH ARTICLE

Open Access

Novel exterior cover design for radiant heat resistance of firefighting robots in large-scale petrochemical complex fires

Jun Fujita[1,5*], Yoshihiro Tamura[2], Hisanori Amano[3], Kazunori Ohno[4] and Satoshi Tadokoro[5]

Abstract

Fires in petrochemical complexes are inaccessible because of the intense radiant heat from flames. Therefore, water cannon robots require radiant heat countermeasures to perform firefighting safely. Conventional radiant heat countermeasures employ a self-spraying method, wherein the water cannon robot requires a water tank of capacity 1.5 m^3 (= 1500 L) to function for 7–8 min in an environment with a 20 kW/m^2 radiation heat. However, the water cannon robot has size limitations because it is transported on one transport vehicle (10 t truck) to the site, and only a tank of capacity ~ 0.02 m^3 can be installed on the robot. To overcome these drawbacks, this study proposes a method that utilizes a mountable radiant heat-resistant exterior cover that works with a small amount of water. The cover is made of radiant heat-shielding fireproof clothing with an aluminum coating that reflects 90% of the radiant heat on the surface and a mist nozzle that sprays water on the back surface. The remaining 10% is removed by the heat of vaporization of water sprayed on the back of the clothing and natural convection. The amount of water required for cooling was reduced to 1/80th of that compared to self-spraying because of the use of the developed cover. The proposed method of radiation reflection via vaporization and natural convection can be employed to protect firefighting robots.

Keywords: Water cannon robot, Radiant heat resistance, Fireproof clothing, Vaporization by mist nozzle, Thermal equilibrium model

Introduction

In recent years, large-scale fires, such as those presented in Table 1, have become a major concern in petrochemical complexes in Japan. Petrol tanks of petrochemical complexes are equipped with sprinklers [1], which can control the extinguishment and spread of small-scale fires. However, in case of large-scale accidents, for example, when the floating roof of an oil tank is shaken and sunk due to an earthquake, the fluid inside the tank may come into contact with air and cause a tank fire [2]. The vicinity of large-scale fire is an environment with high radiant heat and explosion risk.

Deploying human firefighters in such an environment to extinguish fire poses dangers to human life; therefore, a new technique that employs firefighting robots instead of human firefighters is required. A firefighting robot can discharge water from a road just outside a dike surrounding the outer circumference of the oil tank—this is done to efficiently discharge a large amount of water to extinguish the flame. The maximum radiant heat intensity from the flame at this position is estimated to be 20 kW/m^2, according to the "Guidelines for Disaster Prevention Assessment of Petroleum Complexes (March 2013 Extraordinary Disaster Management Office, Fire, and Disaster Management Agency)" [3]. The heat resistance of firefighting suits worn by firefighters is assumed to be

*Correspondence: jun.fujita.3q@nu.mhi.com

[1] Mitsubishi Heavy Industries, LTD, 1-1, Wadasaki-cho 1-chome, Hyogo-ku, Kobe, Hyogo 652-8585, Japan
Full list of author information is available at the end of the article

Table 1 Recent serious disasters in Japan with difficult-to-extinguish fires

Date	Location	Disaster type	Number of casualties	Notes
September 2003 [4, 5]	Idemitsu Kosan Co., Ltd Hokkaido Refinery	Crude oil and naphtha tank fire	0 dead 0 injured	The floating roof sank due to the long-period vibration of the earthquake, and the whole tank caught fire. We had to wait for the contents to burn out while cooling the tank and preventing it from collapsing, and it kept burning for 44 h
March 2011 [6, 7]	Cosmo Oil Co., Ltd Chiba Refinery	LPG tank fire explosion accident	0 dead 6 injured	BLEVE[a] was generated, and the large-scale explosion of the tank occurred successively. It was very difficult to extinguish the fire because of the radiant heat from the flame and the danger of explosion
September 2012 [8]	Nippon Shokubai Co., Ltd Himeji Plant	explosion accident	1 dead 36 injured	An explosion occurred at a chemical plant due to an abnormal temperature rise, and a firefighter died

[a] Boiling liquid expanding vapor explosion (BLEVE): a phenomenon in which a tank ruptures in a state in which a liquid stored in a pressurized container (gas tank) is heated by a fire; the internal pressure of the tank drops rapidly to atmospheric pressure, causing the liquid to boil and become a gas, causing an explosion. If this is a combustible substance and is mixed with air and ignited, the power of the explosion becomes enormous, and the damage becomes even more significant

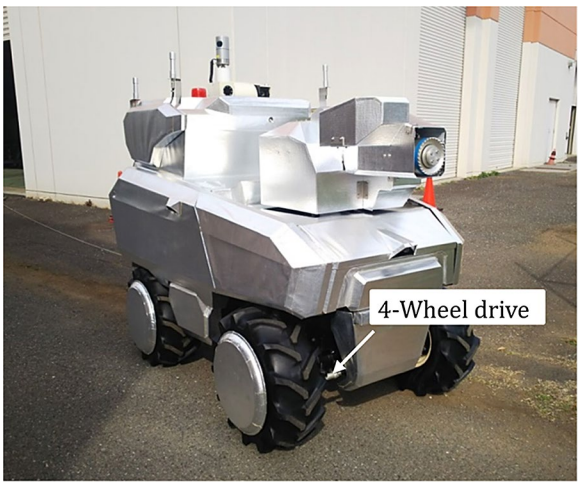

Fig. 1 Water cannon robot

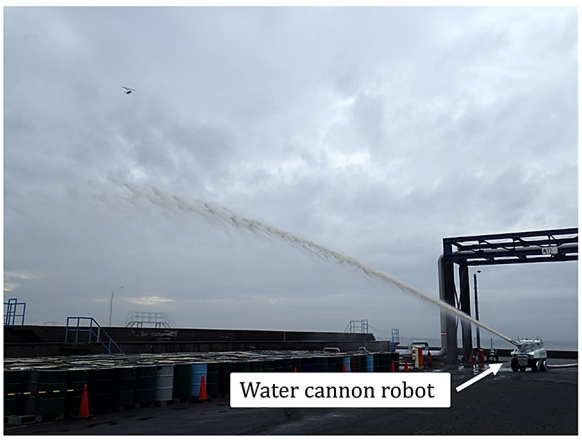

Fig. 2 Water cannon robot in action

approximately 4 kW/m^2; therefore, they cannot endure the radiant heat from the flame. A firefighting robot must be capable of enduring a radiation heat of 20 kW/m^2 to extinguish the fire without direct human intervention.

Figure 1 shows the water firefighting cannon robot developed by the Fire and Disaster Management Agency, which can respond to fires in petrochemical complexes. Figure 2 shows the situation where the water cannon robot discharges water from the vicinity of a dike to the tank. The robot system was deployed at the Ichihara Fire Department in Japan in April 2019. In addition to the water cannon robots, the deployed firefighting robot systems include a hose-laying robot, flying-type inspection robot, traveling-type inspection robot, and corresponding control devices. The firefighting robot system is mounted on one transport vehicle (10 t truck) and dispatched to the site. The truck size is decided based on the size of the fire station it is stored at and the road that it could pass through. For mounting all firefighting robot systems on the transport vehicles, the size of the water cannon robot was limited to 1.5 m in width and 2000 kg in mass.

The deployed water cannon robot has a water discharge capacity of 4 m^3/min and discharges sufficient water by connecting to a fire hose (150 A) with a diameter of 150 mm. The weight of the fire hose is 2 kg/m, and the total weight of the fire hose when the length to be laid was 300 m was 600 kg. Therefore, the water-discharging robot cannot move to the water-discharging position by

pulling the fire hose, as the fire hose can be damaged by being caught in the corner or rubbed. Therefore, after the water cannon robot reaches the water-discharge position, the hose-laying robot lays a hose between the water cannon robot and the water source [9]. After the water cannon robot heading to the water-discharge position enters the highly radiant heat environment in the vicinity of the water-discharge position, it takes 7–8 min for the hose-laying robot to finish laying the hose to the water source and send water. During this time, the idle water cannon robot must withstand the radiant heat from the flame.

Self-protection sprinkling is an existing radiant heat-resistant technology used in firefighting equipment in which approximately 0.2 m^3/min of water is sprinkled on oneself. The technology allows part of the water supplied from the fire hose to be sprinkled on oneself. However, this technology cannot be used while the water cannon robots wait for the hose-laying robot to finish laying the hose. Therefore, it is conceivable to mount a tank capable of holding 1.5 m^3 (mass 1.5 t) of water, which is necessary for 7–8 min of self-sprinkling on the water cannon robot. However, such a water tank cannot be mounted on a robot with width $\leq$ 1.5 m and mass $\leq$ 2000 kg.

Hence, this study proposes a radiant heat-resistant exterior cover mountable on a robot to cope with a high radiant heat of 20 kW/m^2 using far less water for self-protection than the existing technology. This lightweight exterior comprises a frame, radiant heat-shielding cloth, and spray nozzle. Approximately 90% of the heat rays are reflected at the surface of the radiant heat-shielding cloth. The remaining heat passing through the fiber is removed by the heat of vaporization of water retained by the spray. Thus, the radiant heat received by the robot can be reduced to a level where cooling is possible by replacing air with natural convection flowing through the robot opening. Because the amount of water required for self-cooling can be reduced to 1/80th of that compared to conventional self-protection sprinkling, the tank size for loading water can also be reduced.

Practical examples and related research on radiation resistance

Several equipment and robots that can operate in a radiant heat environment have been developed for practical use. Most of them comprise a self-protection sprinkling system where water is directly poured on them, or a water curtain is placed between the robot and flame. Both methods require a large amount of water and use water supplied from the outside or a tank installed on the device. In the latter, a large vehicle is equipped with a water tank of several thousand to tens of thousands of liters for sprinkling [10, 11].

The externally supplied water is used in a fire engine equipped with a self-protection sprinkling function (Fig. 3) and a water discharge robot. Until the water is supplied, the system is operated within a range that can withstand heat irradiation. Some water cannon robots connect fire hoses and move by rubbing and discharging water while receiving water supply from a pump or water source [12]. These are assumed to be operated under limited conditions, such as short-distance linear movement using the light and small-diameter fire hoses with a water supply capacity of approximately 0.5 m^3/min.

As a related study to reduce radiant heat from flames other than the general method of using self-protection sprinkling, there is a report on covering the body with a porous material such as a sponge, keeping cooling water supplied to it, and preventing temperature rise by its vaporization heat [13]. In contrast, our proposed method reduces the amount of heat input itself by using reflective materials, and then uses vaporization heat and natural convection to lower the temperature. In [14], there is a report of a study of an idea to cool a robot by mounting liquid nitrogen in a tank and circulating liquid nitrogen

Fig. 3 Self-protection sprinkling system mounted on fire engines (photo courtesy: Yokkaichi City Fire Department and Ichihara City Fire Department)

inside the robot. We believe that our proposed method is suitable for firefighting robots that can be mobilized at any time, because it uses ordinary water, the robot does not need special equipment for liquid nitrogen, and there is no need to manage whether the robot is equipped with enough liquid nitrogen.

This combination reduces the amount of water used and allows the water tank to be smaller, thus making it possible to reduce the size of the robot. The water cannon robot uses a fire hose with a diameter of 150 mm to discharge a large volume of water at 4 m^3/min to extinguish large-scale fires. The fire hose is too heavy and rigid for the water cannon robot to drag. Therefore, a water tank was mounted on the robot for sprinkling water when there was no water supply. A robot of practical size was achieved because the size of the mounted water tank could be reduced due to the radiant heat-resistant exterior cover that required only a small amount of water.

Development of radiant heat-resistant exterior cover

Radiant heat intensity in a petrochemical complex fire

Because the radiation intensity assumed to be received by the robot in a petrochemical complex fire was set at 20 kW/m^2, the radiant heat-resistant exterior cover was designed to withstand this radiation heat intensity. This value was set by the National Research Institute of Fire and Disaster by calculating the amount of radiant heat at the water-discharge position of a water cannon robot in accordance with the "Guidelines for Disaster Prevention Assessment of Petroleum Complexes," [3] assuming fire that can break out in the largest oil tank in Japan of height 25 m and 100 m diameter.

The radiant heat in [3] is a function of flame size, distance from the flame, height relationship with the flame, and combustion substance. The water-discharge position was assumed to be just outside the dike, and one side of the dike was set at 160 m with reference to the layout of an actual petrochemical complex in Japan (Fig. 4). When fire breaks out in an underground tank with a diameter of 100 m containing ethylene, the amount of radiation heat received at the flame end will be 20 kW/m^2 (Fig. 5). However, during an actual fire, water is not discharged from the immediate vicinity of the flame but in the best position considering various conditions within the range of the water cannon. Assuming that the water-discharge position in the underground tank fire is the dike position, the radiant heat quantity is approximately 12.5 kW/m^2, as seen in the graph in Fig. 5. Therefore, a robot withstanding a radiant heat intensity of 20 kW/m^2 could cope with almost all petrochemical complex fires, including severe scenarios in which the robot operates immediately next to a flame.

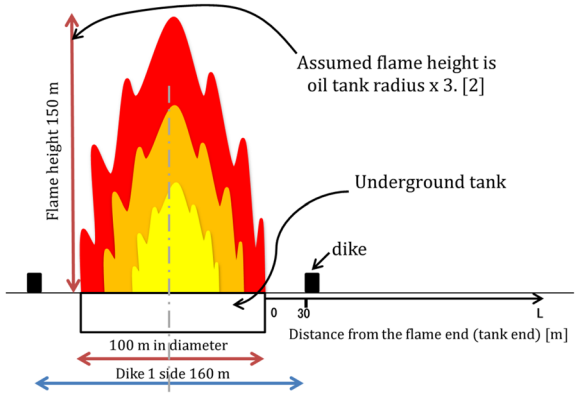

Fig. 4 Dimensional relationship of underground tank fire

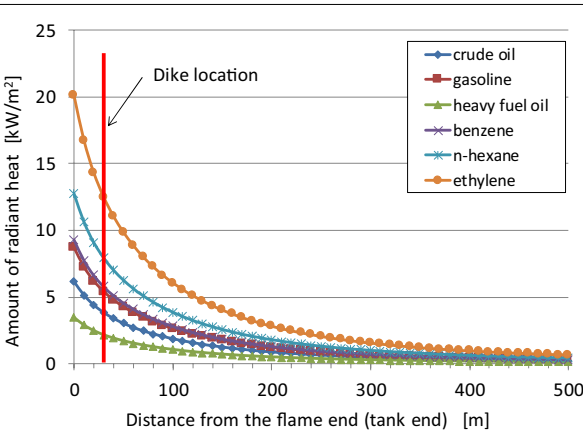

Fig. 5 Radiant heat intensity for distance from the flame end in an underground tank fire

Overview of the radiant heat-resistant exterior cover

The proposed radiant heat-resistant exterior cover uses both reflection and water spray. The thermal equilibrium model is shown in Fig. 6, and the image and cross-sectional schematic diagram are shown in Fig. 7. The radiant heat-resistant exterior cover is made of an aluminum frame covered with radiant heat-shielding fireproof clothing. The front surface (facing the flame side) reflects radiant heat, and the back surface (robot side) is made of reinforcing fibers. The end of the cloth was bonded to the aluminum frame and fixed. The frame uses a pipe with a square cross-section, and the pipe edge is in contact with the back surface of the radiant heat-shielding cloth; thus, the contact is made not by the surface but by the line edge, and the heat conduction to the robot by the contact is reduced as much as possible.

In the thermal equilibrium model for a robot receiving radiant heat from a flame, the heat sources include radiation from the fire R_{FIRE} and heat generated inside

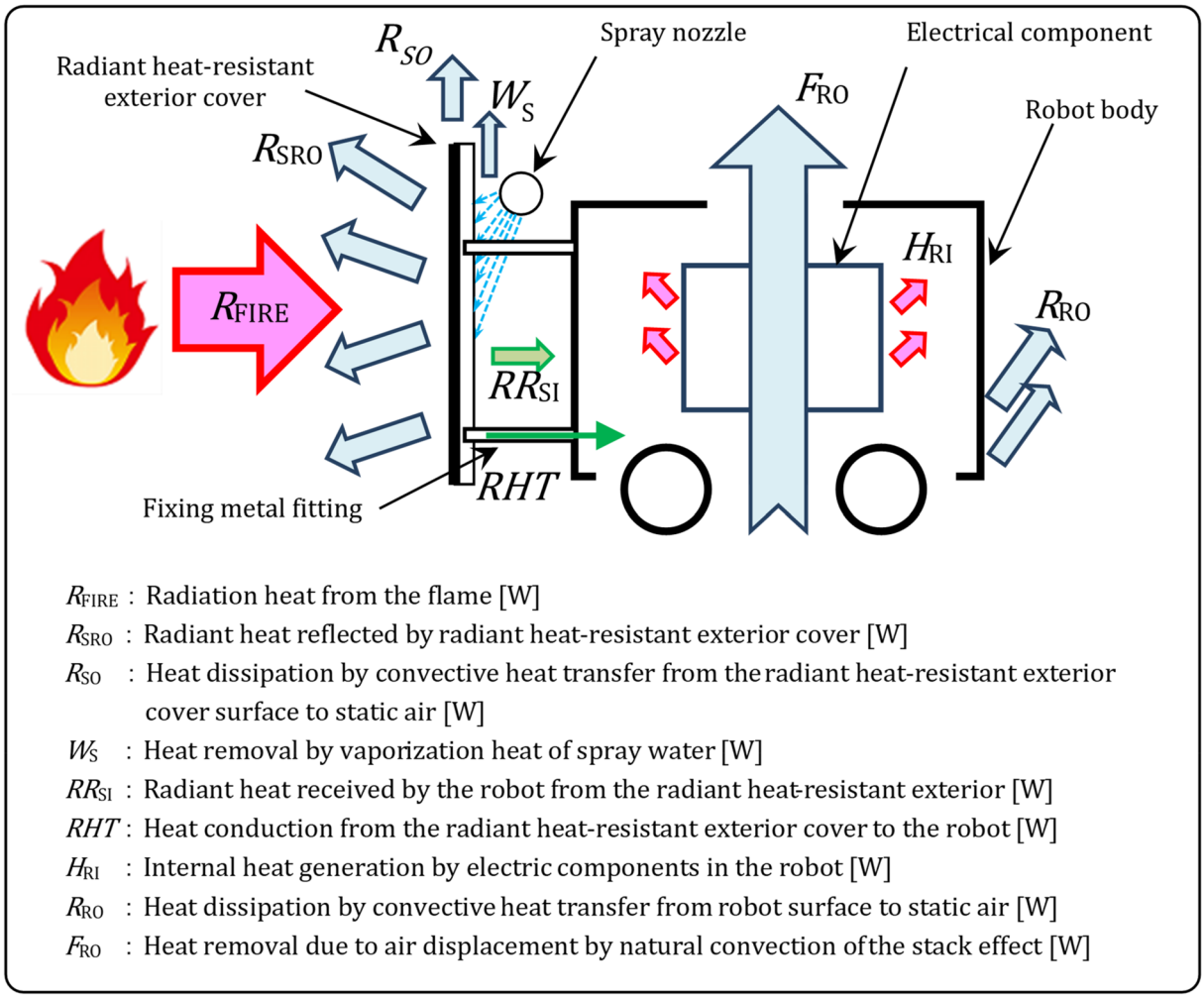

Fig. 6 Thermal equilibrium model of a robot subjected to radiation heat from flames

the robot H_{RI}. R_{SRO} is the heat reflected by the aluminum material of the radiant heat-resistant exterior cover, R_{SO} and R_{RO} are the heat radiated from the radiant heat-resistant exterior cover surface and robot body surface to the atmosphere, respectively; W_S is the heat vaporized by the spray of a small amount of water and F_{RO} is the heat released by air displacement inside the robot by natural convection due to the stack effect (chimney effect). The heat radiated from the flame heats the ground. Still, the heat capacity of the ground is large, and the thermal diffusivity is high, so the temperature of the ground does not rise significantly. Therefore, heat conduction through the tire and heat input to the robot due to radiant heat received from the ground were ignored.

The heat balance equation for this model is then given by Eq. (1).

$$R_{FIRE} + H_{RI} = R_{SRO} + R_{SO} + W_S + F_{RO} + R_{RO} \quad (1)$$

Most of the received heat quantity R_{FIRE} is reflected by the radiant heat-resistant exterior cover R_{SRO}. The remaining is reduced by heat radiation R_{SO} to the atmosphere, and vaporization heat W_S by water spray utilizing water retention on the back surface. For selecting the radiation heat-shielding cloth, the emissivity of DM-1088, ALM1151, and a stainless-steel plate (SUS Plate) was considered. From the measurement results in Table 2, DM-1088 (manufactured by GENTEX), which reflected more radiant heat because of its low emissivity, was selected.

The relationship between emissivity and reflectivity is expressed as reflectivity = 1 − emissivity − transmissivity. Here, the transmissivity is 0 because the fireproof fabric is thick enough not to pass light (infrared rays).

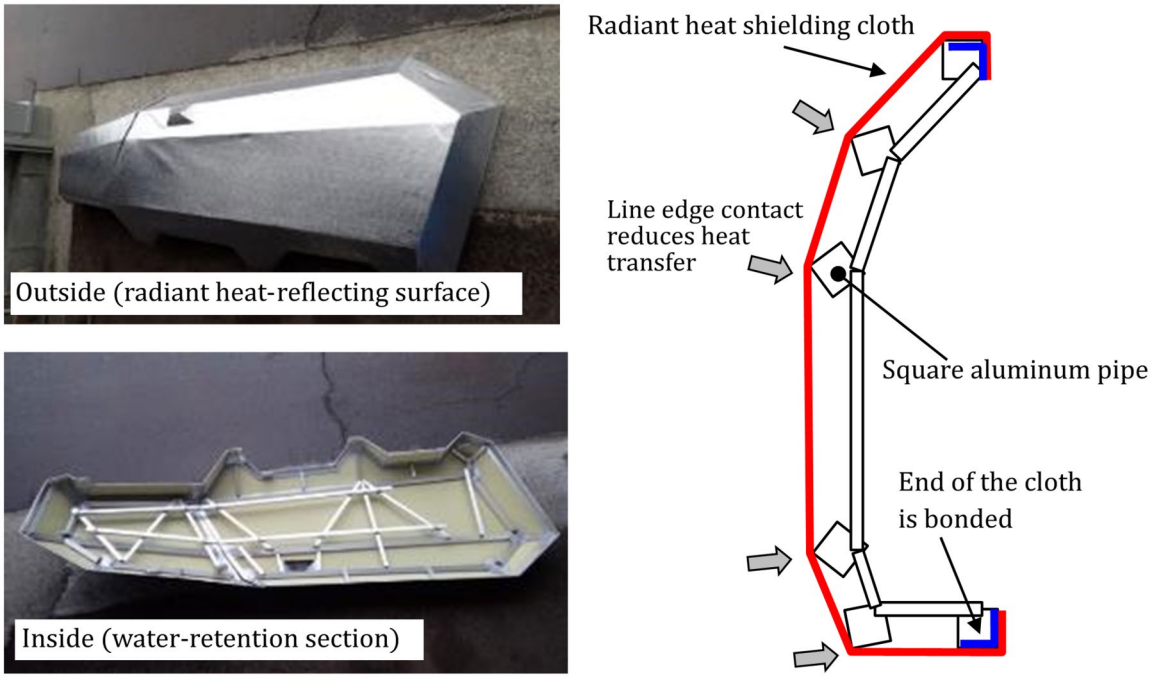

Fig. 7 Image of the developed radiant heat-resistant exterior cover and cross-sectional schematic diagram

Table 2 Emissivity measurement result of fire protection cloth

Number of measurements	SUS plate front surface	SUS plate back surface	ALM1151 front surface	ALM1151 back surface	DM-1088 front surface	DM-1088 back surface
1st	0.140	0.140	0.090	0.840	0.050	0.890
2nd	0.140	0.140	0.080	0.850	0.050	0.880
3rd	0.140	0.140	0.090	0.840	0.050	0.890
Average	0.140	0.140	0.087	0.843	0.050	0.883

The heat balance equation of the radiant heat-resistant exterior cover in Fig. 6 can be expressed using Eq. (2), where the left side is the heat input, and the right side is the heat removal.

$$R_{\mathrm{FIRE}} = R_{\mathrm{SRO}} + R_{\mathrm{SO}} + W_{\mathrm{S}} + RR_{\mathrm{SI}} + RHT \tag{2}$$

where RR_{SI} is the radiant heat received by the robot from the exterior cover and RHT is the heat conduction from the exterior cover to the robot. $R_{\mathrm{SRO}} + R_{\mathrm{SO}} + W_{\mathrm{S}}$ can be regarded as a reduction effect of radiant heat from the flame by the exterior cover, R_{SRO} is the reflectance, and $R_{\mathrm{SO}} + W_{\mathrm{S}}$ varies depending on the spray condition of the rear surface.

In addition, $RR_{\mathrm{SI}} + RHT$ is the amount of heat that the robot receives from the flame after passing through the exterior cover. If the internal heat H_{RI} of the robot is added, the heat balance equation of the robot can be expressed using Eq. (3), where the left side is the heat input, and the right side is the heat removal.

$$RR_{\mathrm{SI}} + RHT + H_{\mathrm{RI}} = R_{\mathrm{RO}} + F_{\mathrm{RO}} \tag{3}$$

In Fig. 6, RR_{SI} and RHT are the internal heat transfers in the model, and eliminating them using Eqs. (2) and (3) results in the heat balance in Eq. (1) for the entire model.

Robot heat balance equation considering the effect of radiant heat reduction from flames using the radiant heat-resistant exterior cover

The calculation of the heat balance equation

When designing an actual robot, one needs to consider the radiant heat balance equation in Eq. (3) and balance the heat removal on the right side with respect to the heat input on the left side. The formula for each term is as follows:

- RR_{SI} [W]: radiant heat received by the robot from the exterior cover is given as

$$RR_{SI} = \frac{1}{\frac{1}{F_{SB}} + \left(\frac{1}{\varepsilon_S} - 1\right) + \frac{A_S}{A_B}\left(\frac{1}{\varepsilon_B} - 1\right)} \sigma\left(T_S^4 - T_B^4\right) A_S \tag{4}$$

A_S: area of radiant heat-resistant exterior cover backside heat dissipation surface [m^2]; A_B: area of the heat-receiving surface of the robot body [m^2]; ε_S: emissivity of the radiant heat-resistant exterior cover back surface; ε_B: emissivity of the robot body; F_{SB}: form factor; T_S: temperature of the radiant heat-resistant exterior cover back surface [K] (calculated in Eq. (4) at absolute temperature); T_B: robot body temperature [K] (calculated in Eq. (4) at absolute temperature); σ: Stefan–Boltzmann constant.

- RHT [W]: heat conduction from radiant heat-resistant exterior cover fixing bracket to the robot is calculated as follows.

$$RHT = \mathrm{k} \times \frac{A}{L} \times (T_S - T_B) \tag{5}$$

k: thermal conductivity of the thermally conductive body [W/mK]; A: cross-sectional area of the thermally conductive body [m^2]; L: length of the thermally conductive body [m]; T_S: temperature of the radiant heat-resistant exterior cover back surface [°C]; T_B: robot body temperature [°C].

- H_{RI}[W]: Internal heat generation by the electric components mounted on the robot is calculated based on the power consumption. The motor driver radiates 20% of the power consumption, and the other electric components radiate 100% of the power consumption.
- R_{RO}[W]: convective heat transfer from the robot surface to the air is calculated as follows and is derived experimentally:

$$R_{RO} = KA(T_B - T_A) \tag{6}$$

K: convective heat transfer coefficient [W/m^2K]; A: heat dissipation area [m^2]; T_A: outside air temperature [°C]; T_B: robot body temperature [°C].

- F_{RO}[W]: heat removal due to air replacement by natural convection in the stack effect is calculated from the constant pressure specific heat of dry air as follows:

$$F_{RO} = C_p \cdot \rho q (T_I - T_A) \tag{7}$$

C_p: constant pressure specific heat of dry air [J/kgK]; ρ: dry air density [kg/m^3]; q: airflow rate [m^3/s]; T_A: outside air temperature [°C]; T_I: robot internal temperature [°C].

Here, the airflow rate q was calculated using Eq. (8) as natural convection generated by the stack effect in which buoyancy is generated and raised in the high-temperature gas in the robot, and low-temperature air is supplied from the lower part when the robot is regarded as a chimney.

$$q = CA\sqrt{2gh\frac{T_I - T_A}{T_I}} \tag{8}$$

C: discharge coefficient; A: flow area [m^2]; g: gravitational acceleration [m/s^2]; h: height or distance [m]; T_I: robot inside temperature [K] (calculated in Eq. (8) at absolute temperature); T_A: outside air temperature [K] (calculated in Eq. (8) at absolute temperature).

The convective heat transfer coefficient K and discharge coefficient C were calculated from the radiation heat transfer experiment (described in "Radiation heat-transfer experiment" section). The experiment was conducted using a radiant heat source and a simplified model of a robot equipped with a radiant heat-resistant exterior cover to measure the required temperature.

Estimating the convective heat transfer coefficient K

When there is no internal heat generation or natural convection in the robot, i.e., $F_{RO} = H_{RI} = 0$, Eq. (3) can be expressed as follows:

$$RR_{SI} + RHT = R_{RO} \tag{9}$$

Equation (9) is also valid for the simplified model of the robot used in the radiation heat transfer experiment. The convective heat transfer coefficient K can be derived by calculating RR_{SI}, RHT, and R_{RO} using the radiation heat-transfer experiment results under the conditions in Eqs. (4)–(6) and substituting them in Eq. (9).

Estimating the discharge coefficient C

In a situation where the robot has a vent, and the internal air is replaced by natural convection, Eq. (3) can be expressed as Eq. (10) because $H_{RI} = 0$ when there is no internal heat generation.

$$RR_{SI} + RHT = R_{RO} + F_{RO} \tag{10}$$

Equation (10) is also valid if the simplified model of the robot used in the radiation heat transfer experiment has a vent at the top and no internal heat generation. Using the results of the radiation heat-transfer experiment and convective heat transfer coefficient K estimated in "Estimating the convective heat transfer coefficient K" section, RR_{SI}, RHT, R_{RO} are calculated from Eqs. (4)–(6), and F_{RO} is calculated using Eq. (11) by substituting Eq. (8) into Eq. (7).

$$F_{\mathrm{RO}} = C_{\mathrm{p}} \cdot \rho q \cdot T = C\left(C_{\mathrm{p}} \cdot \rho \cdot A\sqrt{2gh\frac{T_{\mathrm{I}} - T_{\mathrm{A}}}{T_{\mathrm{I}}}}\right)(T_{\mathrm{I}} - T_{\mathrm{A}}) \quad (11)$$

The discharge coefficient C is then estimated by substituting Eq. (11) in Eq. (10).

Radiation heat-transfer experiment

Outline of the experiment

The radiation heat-transfer experiment was performed by simulating the conditions under which a robot equipped with a radiant heat-resistant exterior cover receives 20 kW/m^2 radiative heat from a flame. The experiment had two objectives. The first is the measurement of temperature data to estimate the convective heat transfer coefficient K and discharge coefficient C in Eq. (3). The second is to evaluate the amount of heat received by the robot under the spraying conditions on the back surface of the radiant heat-resistant exterior cover.

A panel heater was used to create a radiant heat environment of 20 kW/m^2. For the radiant heat-resistant exterior cover, we prepared a structure that can inject water to simulate the spraying on the back surface using the selected DM-1088.

The simplified robot model (a cube with one side equal to 200 mm) has an openable vent at the top to reproduce the presence or absence of air displacement by natural convection of the stack effect. The internal heat generated from the robot's electrical components can be added as parameters in the actual robot design and was not considered in the simplified model. The thermocouples were placed in various places inside the simplified model, and the temperature was measured by changing the conditions of water spraying and opening and closing of the vent during irradiation with the radiant heat. Figure 8 shows the schematic diagram of the experimental equipment. Table 3 shows the specifications of the equipment used for the experiment, and Fig. 9 shows the radiation heat-transfer experiment setting. This experiment was performed with the support of the National Research Institute of Fire and Disaster, including equipment and materials.

The details of the equipment and conditions of the experiment are as follows. The radiation heat-transfer experiment was performed indoors under no-wind

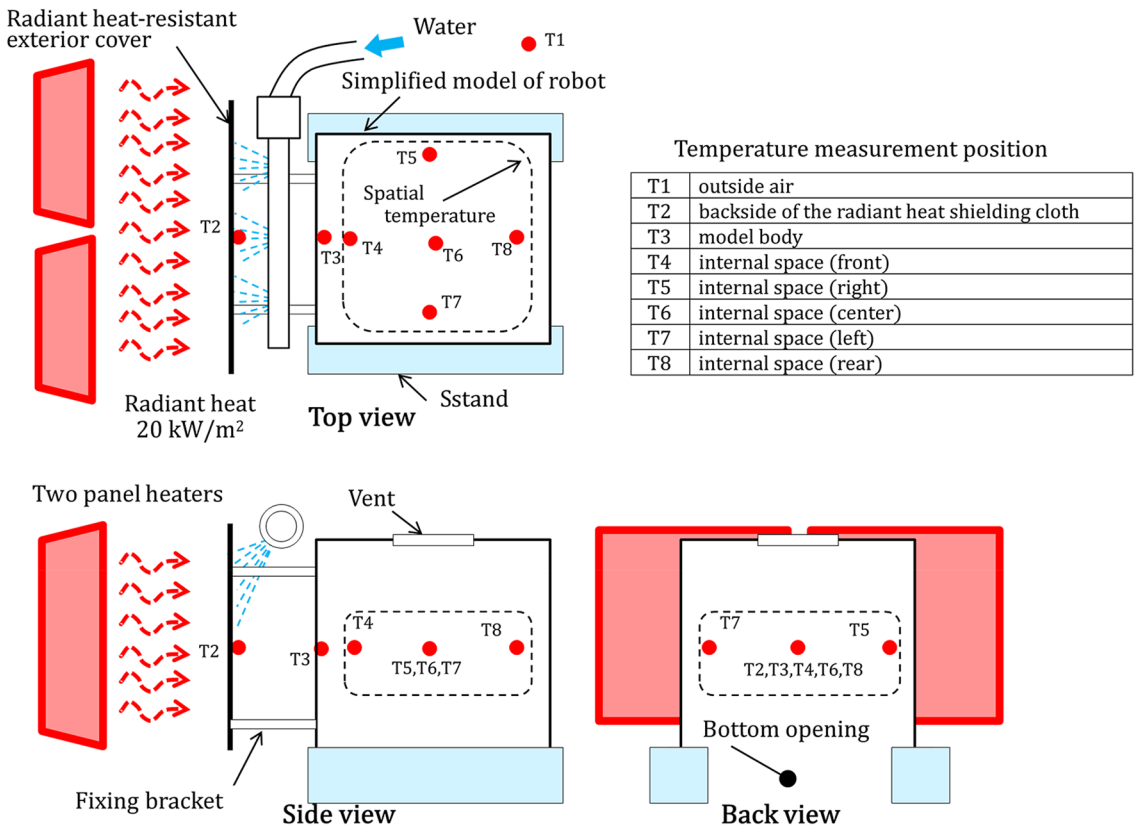

Fig. 8 Schematic diagram of the radiation heat-transfer experiment using a simplified robot model with the radiant heat-resistant exterior cover

Table 3 Equipment using radiation heat-transfer experiment

Equipment	Specifications	Notes
Heat source	Panel Heater (OMEGALUX: QH-121260-T) Heating surface dimension: 300 mm square	Rented from the Fire and Disaster Management Agency
Heat flux meter	Radiometer (Tokyo Seiko Inc.: RE-IV) Output: approx. 70 mV, 25 kW/m^2 Cooling: water cooling	Rented from the Fire and Disaster Management Agency
Data logger	data acquisition unit (Yokogawa Electric Corporation: DA100-11-1M/M1) Module: DU100 (T/C·Voltage), DT300 (Ethernet)	
Thermocouple	Sheath thermocouple (Okazaki Manufacturing company: TYPE-K (Class1) Sheath diameter: 1.0 mm	

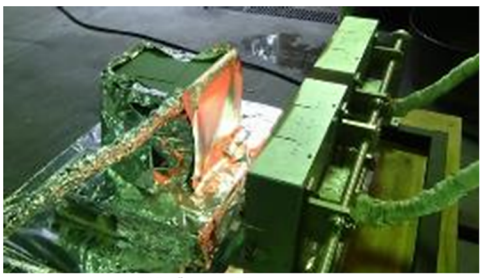

Without Top vent

With Top Vent

Scene of water spraying to the backside of the radiant heat-shielding cloth

Fig. 9 Setting of the radiation heat transfer experiment

conditions. The simplified robot model has a cubic structure with one side of 200 mm formed by combining carbon steel plates with a thickness of 1.6 mm and has a square vent (area: approx. 5929 mm^2) of approximately 77 mm on the upper surface (Fig. 9). The natural convection inside the simplified model of the robot can be adjusted by opening and closing the vent with the cover. The bottom surface was fully open to ensure an air inflow path. The thermocouple was fixed at positions T1 to T8, as shown in Fig. 8, and the temperature was measured and recorded using a data logger. A selected radiation heat-shielding cloth, DM-1088, was mounted as a radiant heat-resistant exterior cover on a heater irradiation surface in front of a simplified model of the robot. The four corners of the radiant heat-shielding cloth were fixed to the simplified model of the robot using stainless steel fixing fittings (cylinder with a diameter of 10 mm and length of 30 mm). An aluminum foil was used to shield surfaces without a radiant heat-resistant exterior cover, such as the side surface of a simplified model of the robot, from heat input due to the radiated heat of the heater.

Preparation of the 20 kW/m^2 radiant heat environment

A radiant heat environment of 20 kW/m^2 was reproduced with a panel heater in preparation for the radiation heat-transfer experiment. Two panel heaters were arranged at

an appropriate distance to obtain a uniform radiant heat distribution in front of the panel heater. The radiant heat intensity at the front of the panel heater was measured using a heat flux meter, and the position (distance from the panel heater) capable of radiating 20 kW/m^2 radiant heat was determined. The radiation heat-transfer experiment was performed by arranging a simplified model of a robot with a radiant heat-resistant exterior cover in this position.

A heat source was prepared such that the distance between the centers of the two panel heaters was 360 mm, and a position 195 mm away from the panel heaters could reproduce a radiant heat environment of 20 kW/m^2. Figure 10 shows the results of the radiant heat measured at 195 mm. In the area where the 200 mm simplified robot model was placed, the environment would be irradiated with a maximum of 20 kW/m^2 and a minimum of 17.8 kW/m^2 of radiant heat, 11% lower than the target.

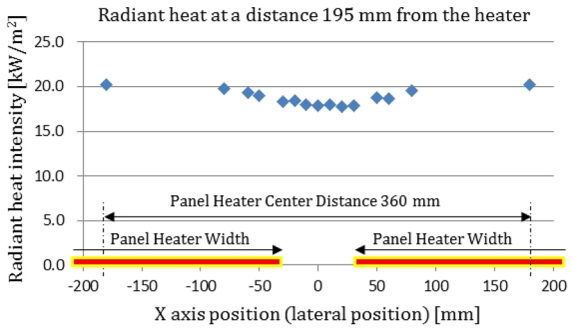

Fig. 10 Radiant heat at a distance of 195 mm from the heater

This 11% reduction in the radiation heat quantity should be considered during the thermal design. In "Robot heat balance equation considering the effect of radiant heat reduction from flames using the radiant heat-resistant exterior cover" and "Experimental results and estimation of convective heat transfer coefficient and discharge coefficient" sections, the parameters related to the robot-to-air radiation R_{RO} calculated from experimental data, and the heat removal F_{RO} by natural convection, are not affected by this 11% reduction in radiant heat exposure because they identify the coefficients related to heat balance. In contrast, when designing the actual robot, in "Design of water cannon robot with radiant heat-resistant exterior cover based on the radiation heat-transfer experiment" section, the radiant heat RR_{SI} the robot receives from the radiant heat-resistant exterior cover and the heat-transfer RHT received from its fixing bracket were calculated using the experimental temperature measurement results, assuming that the 11% of the actual measured value was added with heat. The overall correction to the minimum value of radiant heat radiated in the experiment was performed by turning the thermal design to the safe side.

Radiation heat-transfer experiment

The conditions for the radiation heat-transfer experiment are listed in Table 4. The purpose of the experiment is to measure the temperature data to estimate the convective

Table 4 Experimental conditions for radiative heat irradiation

Experiment symbol[a]	Vent status	The initial state of the radiation heat shielding cloth	Intermittent spraying pattern
(e1) (OD-N)	Open	Dry	None
(e2) (CD-N)	Close	Dry	None
(e3) (OW-N)	Open	Wet enough	None
(e4) (OD-1/30)	Open	Dry	Spray 10 s, stop 290 s Duty cycle: 1/30
(e5) (OD-1/20)	Open	Dry	Spray 3 s, stop 57 s Duty cycle: 1/20
(e6) (OD-1/60)	Open	Dry	Spray 1 s, stop 59 s Duty cycle: 1/60
(e7) (OW-C)	Open	Wet enough	Continuous

Water supply volume: approx. 0.001 m^3/min Water supply to the back of the radiant heat shielding cloth by turning the pump on and off

[a] (e○) (△□ – ▼)

○: experiment number

△: vent status O (open), C (close)

□: Initial state of the radiation heat shielding cloth D (dry), W (wet)

▼: intermittent spraying pattern

N (none), duty cycle, C (continuous)

heat transfer coefficient K and discharge coefficient C necessary for the calculation of the heat balance in Eq. (3) of the robot and evaluate the quantity of heat received by the robot during spraying on the rear surface of the radiation heat-shielding cloth. We reproduced the conditions with the vent closed and opened without water spray for measuring the temperature and performed the experiments as experiment numbers (e2) and (e1), respectively. For evaluating the received heat, the vent was opened under the assumption of natural convection, as in the case of an actual robot, and the experiments (e3) to (e7) were performed under various spraying conditions. Experiment (e3) is performed under the condition that the back of the radiant heat-shielding cloth is sufficiently moistened beforehand and has not been sprayed since then. In (e4) to (e6), continuous feed water was supplied by three intermittent spraying conditions to reduce the amount of water used, and irradiation was performed until thermal equilibrium was reached. In (e7), the experiment was performed with continuous spraying instead of intermittent spraying. To ensure that the temperature of the water sprayed on the back surface of the radiation heat-shielding cloth equals the outside air temperature, water stored in a container of approximately 0.05 m^3 for 4 h or more was used, and water was sprayed using a small pump. In the experiment, a small amount of water was blown out from multiple small-diameter holes on the side surface of the pipe, and the spray was simulated by hitting the back surface of the radiation heat-shielding cloth (see Fig. 9, right). The total flow rate measured from multiple holes was approximately 0.001 m^3/min.

Experimental results and estimation of convective heat transfer coefficient and discharge coefficient

Results of radiation heat-transfer experiment

A radiant heat-transfer experiment was performed using a panel heater as a radiant heat source. The experimental results are shown in Table 5. Figures 11, 12, 13 and 14 show the temperature measurements performed using thermocouples. The sampling period of the measurements was 1 s. The average values measured during the different periods are indicated by yellow hatching in the graph. We used the data from the last part of the measurement, which is considered stabilized under each measurement condition. The averages were calculated using the data for 500 s, but experiment (e4) was calculated using the data for 900 s. The reason is that the spray pattern in the experiment (e4) has a cycle time of 5 min, which is five times longer than the other conditions, and the temperature fluctuation on the backside of the radiant heat-shielding fabric is also large; therefore, 500 s of data is too short for correct average calculation. The data for three cycles in the last part were used to calculate the average to evaluate the experimental results correctly.

The experimental results show the following.

- Upon receiving 20 kW/m^2 radiant heat, the backside of the radiant heat-shielding fabric is heated to approximately 100 °C.
- Opening the vent on the upper part of the simplified robot model replaces the air inside the model by natural convection, which lowers the temperature inside the model.
- When the backside of the radiation heat-shielding cloth receiving radiation heat is supplied with sufficient water, the temperature of the backside of the cloth increases from approximately 50 °C to approximately 100 °C, more slowly than without water. (It was visually confirmed that steam emitted from the radiant heat-shielding cloth when the temperature exceeded 50 °C was due to vaporization heat.)
- When water was sprayed on the backside of the radiation heat-shielding cloth, the temperature on the backside of the cloth reduced. After the spray was

Table 5 Experimental result

Experiment symbol	Period for calculating the average temperature (s)	Outside air (°C)	The back surface of radiation heat shielding cloth (°C)	Simplified model of robot (°C)	Air in the simplified robot model: 5 points average temperature (°C)	Difference between the average air in the model and the outside air (°C)	Fig. number
(e1) (OD-N)	1370–1870	18.65	96.96	50.32	29.57	10.92	Figure 11
(e2) (CD-N)	2500–3000	18.25	95.78	52.37	34.96	16.71	Figure 11
(e3) (OW-N)	626–1126	18.37	69.42	34.47	24.74	6.38	Figure 12
	2500–3000	17.56	100.93	49.11	27.06	9.49	Figure 12
(e4) (OD-1/30)	4100–5000	15.83	44.34	26.75	21.34	5.50	
(e5) (OD-1/20)	2000–2500	17.21	38.16	24.46	21.53	4.323	
(e6) (OD-1/60)	2000–2500	17.08	45.86	27.37	22.56	5.48	Figure 13
(e7) (OW-C)	2000–2500	17.00	20.31	19.53	20.12	3.12	Figure 14

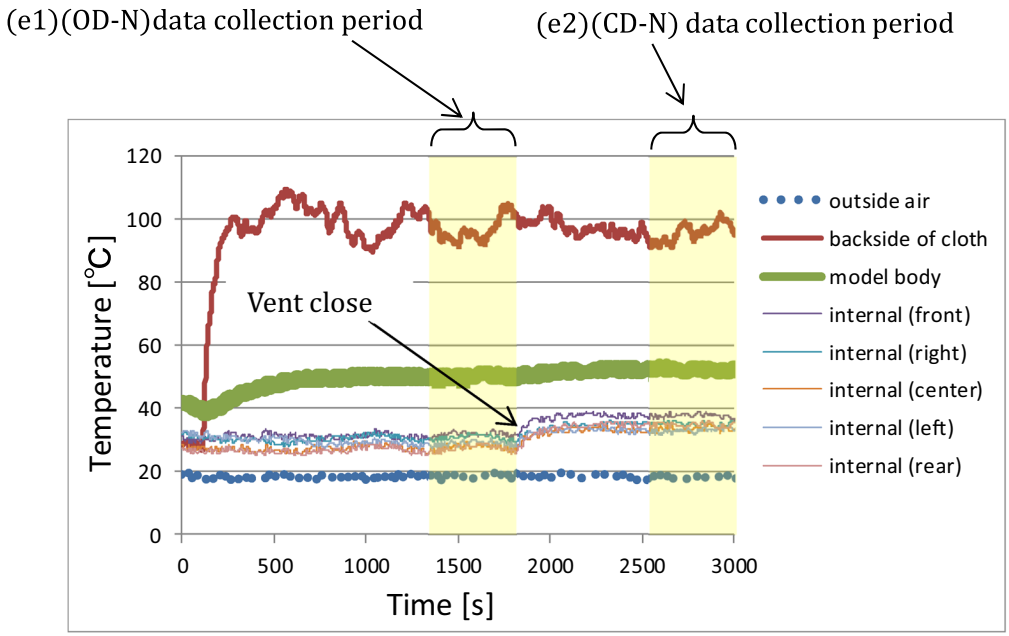

Fig. 11 Temperature measurement results by thermocouples. (e1) (OD-N), (e2) (CD-N)

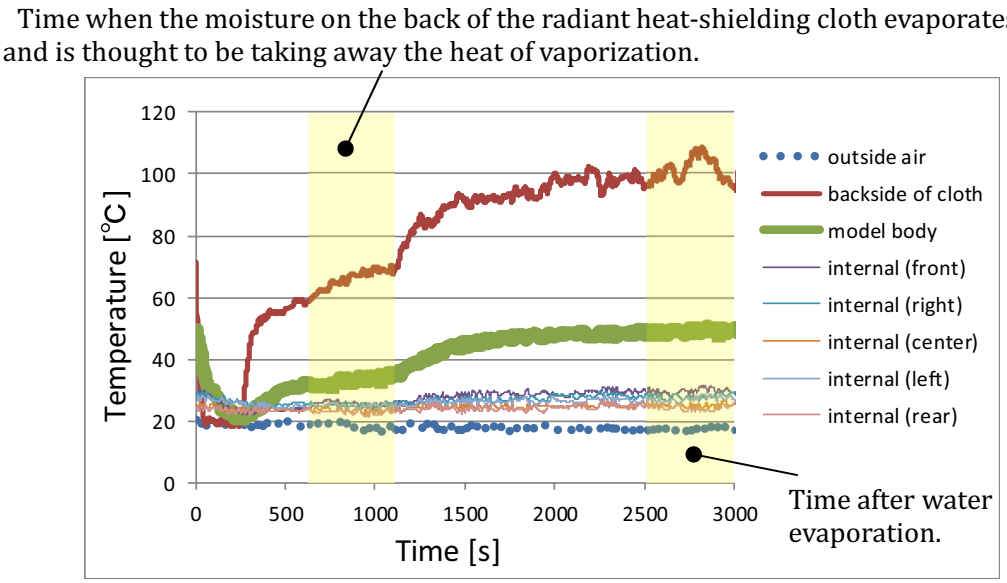

Fig. 12 Temperature measurement results by thermocouples. (e3) (OW-N)

stopped, the temperature increased gradually from approximately 50 °C, as in the case when the radiation heat-shielding cloth is heated from the state of water retention.

- The continuous spray lowered the temperature inside the model the most, and the temperature difference from the outside air temperature was 3.2 °C. Among the intermittent sprays tested, the

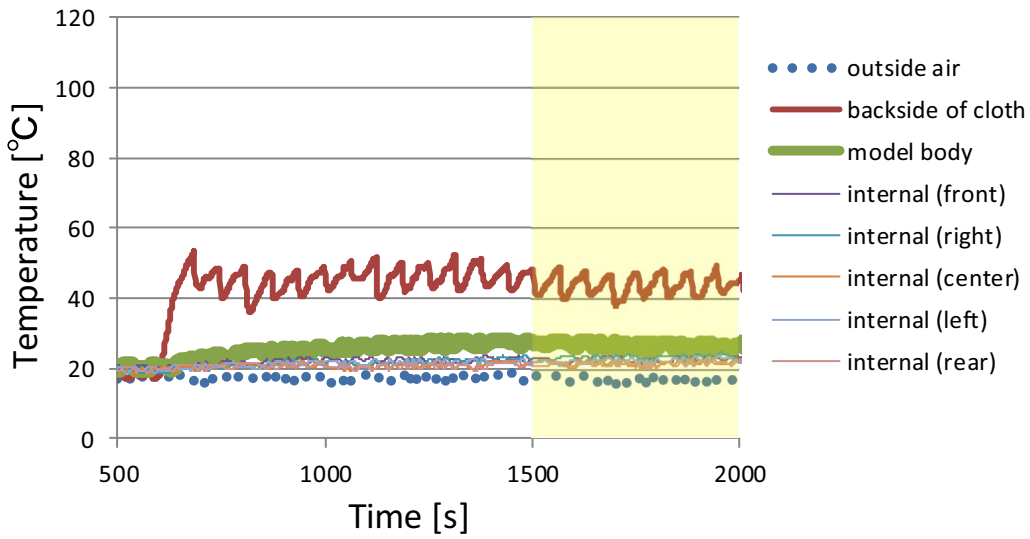

Fig. 13 Temperature measurement results by thermocouples. (e6) (OD-1/60)

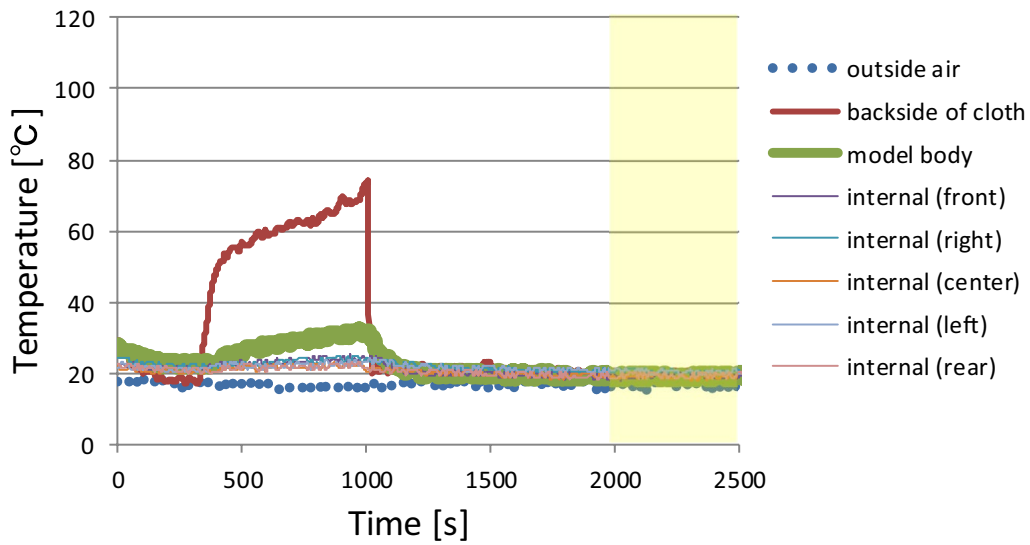

Fig. 14 Temperature measurement results by thermocouples. (e7) (OW-C)

1/20 duty cycle that sprays for 3 s and then stops for 57 s reduced the temperature inside the model the most, and the temperature difference from the outside air temperature was 4.0 °C.

- The 1/60 duty cycle, which sprays for 1 s and then stops for 59 s and saves the highest water volume, increased the temperature by only 5.3 °C compared with the outside air temperature.

Estimation of convective heat transfer coefficient K

The convective heat transfer coefficient K is estimated in "Estimating the convective heat transfer coefficient K" section, using experiment (e2) without natural convection, as follows:

The radiant heat RR_{SI} received by the simplified robot model from the rear surface of the radiant

heat-resistant exterior cover was calculated by substituting the following values into Eq. (4).

$A_S = A_B = 0.04$ m^2: size of the experimental equipment. $\varepsilon_S = 0.883$: measurement results in Table 2. $\varepsilon_B = 0.9$: general value of the painted steel plate surface. $F_{SB} = 1$: for two opposing surfaces, $T_S = 95.78 + 273.15$ K and $T_B = 52.37 + 273.15$ K: experiment (e2) in Table 5. $\sigma = 5.67 \times 10^{-8}$ W/m^2K^4: Stefan–Boltzmann constant

$$RR_{SI} = 13.309 \approx 13.3W \tag{12}$$

The heat conduction *RHT* from the radiant heat-resistant exterior cover fixing bracket to the simplified robot model was calculated by substituting the following value into Eq. (5).

k = 16.3 W/mK: stainless steel property. $A = 3.14 \times 10^{-4}$ m^2 and L = 0.03 m: size of the experimental equipment. $T_S = 95.78$ °C and $T_B = 52.37$ °C: experiment (e2) in Table 5.

$$RHT = 7.4098 \approx 7.41W \tag{13}$$

The heat radiation R_{RO}[W] from the surface of the simplified model of the robot to the air was calculated by substituting the following values into Eq. (6) under the following conditions.

- Because the bottom surface of the model is open, the heat radiation surfaces have five surfaces: front, back, left, right, and top.
- It is assumed that the surface (heat radiation surface to outside air) temperature of the simplified robot model is equal to the average temperature inside the model.

K: unknown to be estimated. A = 0.2 m^2: the five surface areas of the experimental equipment. $T_A = 18.25$ °C and $T_B = 34.96$ °C: experiment (e2) in Table 5.

$$R_{RO} = 3.342K \approx 3.34KW \tag{14}$$

We substitute these results into (9) to estimate the convective heat-transfer coefficient *K* W/m^2K.

$$K = 6.20 W/m^2K \tag{15}$$

The convective heat-transfer coefficient *K* is approximately 5–10 in still air; the estimated values from the temperature measurements obtained in the experiment do not deviate significantly from the ground truth.

Estimation of discharge coefficient *C*

The estimation of the discharge coefficient *C* in "Estimating the discharge coefficient C" section, using experiment (e1) with natural convection by the vent opening, is shown below. R_{RO} was calculated using the convective heat-transfer coefficient *K* estimated in "Estimation of convective heat transfer coefficient K" section.

The radiant heat RR_{SI} received by the simplified robot model from the rear surface of the radiant heat-resistant exterior cover was calculated by substituting the following values into Eq. (4).

$T_S = 96.96 + 273.15$ [K] and $T_B = 50.32 + 273.15$[K]: experiment (e1) in Table 5.

$$RR_{SI} = 14.25 \approx 14.3[W] \tag{16}$$

The heat conduction *RHT* from the radiant heat-resistant exterior cover fixing bracket to the simplified robot model was calculated by substituting the following values into Eq. (5).

$T_S = 96.96$ °C and $T_B = 50.32$ °C: experiment (e1) in Table 5.

$$RHT = 7.961 \approx 7.96[W] \tag{17}$$

The heat radiation R_{RO} from the surface of the simplified model of the robot to the air can be calculated by substituting the following values into Eq. (6).

$T_A = 18.65$ °C and $T_B = 29.57$ °C: experiment (e1) in Table 5.

$$R_{RO} = 13.541 \approx 13.5[W] \tag{18}$$

The heat removal F_{RO} due to air replacement by the natural convection of the stack effect can be calculated by substituting the following value into Eq. (11).

C: unknown to be estimated. $C_p = 1007.7$ J/kgK: constant pressure specific heat of dry air at 23 °C. $\rho = 1.19$ kg/m^3: dry air density at 23 °C. $A = 5.929 \times 10^{-3}$ m^2: experimental equipment vent. g = 9.81 m/s^2: gravitational acceleration. $h = 0.2$ m: experimental equipment height. $T_I = 29.57 + 273.15$ K and $T_A = 18.65 + 273.15$ K: experiment (e1) in Table 5.

$$F_{RO} = 29.210C \approx 29.2CW \tag{19}$$

These results were substituted into Eq. (10) to estimate the discharge coefficient *C*

$$C = 0.30 \tag{20}$$

The estimated discharge coefficient *C* was smaller than the ground truth (approximately 0.6–0.7). This could be because the shape of the simplified robot model with a vent differs from the shape of the chimney, and only the outlet portion has an extremely small opening area. Therefore, airflow due to natural convection could be difficult.

Design of water cannon robot with radiant heat-resistant exterior cover based on the radiation heat-transfer experiment

Using K and C estimated from the results of the radiation heat-transfer experiment, a water cannon robot that can withstand radiation of 20 kW/m^2 is designed using a radiant heat-resistant exterior cover adopting the spray pattern in experiment (e6), requiring the least amount of water.

The main design conditions for the water cannon robot are as follows: the outside temperature is assumed to be 45 °C, which is the highest temperature under the scorching midsummer sun in Japan. The robot is approximately 1.4 m wide, 2 m long, and 1 m high. The heat-receiving area is assumed to be maximum when irradiated from the robot's upper right (or left) oblique. It is assumed that the internal heat generation of the electric components mounted on the robot is 20% of the motor driver's power consumption and 100% of the other components. The development goal is to reduce the robot's internal temperature to 60 °C or less and select and mount the equipment to withstand this temperature. The design conditions are listed in Table 6.

In designing the water cannon robot, as shown in Table 6, it is necessary to satisfy the heat balance Eq. (3) so that the inside temperature of the water cannon robot is 60 °C or less at an outside air temperature 45 °C. Owing to the limited capacity of the battery mounted on the water cannon robot, the design policy was to avoid forced ventilation. Among the various items in the heat balance Eq. (3), the increase in the air substitution quantity due to the stack effect, as a quantity that can be handled in the design of the water cannon robot, was examined to increase the cooling effect, and F_{RO} was set as a development parameter.

Each item in Eq. (3) in the robot design is described below.

Calculation of RR_{SI} is performed under the following assumptions.

- A radiant heat-resistant exterior cover receives radiant heat from flames, and an increase in temperature provides radiant heat to the robot body. Therefore, a maximum area of 3.71 m^2 was assumed to receive oblique irradiation.
- It is assumed that the result of the experiment (e6), in which the temperature on the back surface of the radiant heat shielding cloth is 28.8 °C higher than the ambient temperature (which can be calculated as 45.8 − 17.08 °C), will be reproduced if the intermittent water spray under the conditions of the experiment (e6) is performed on the actual robot. In other words, the temperature of the back surface of the radiant heat shielding cloth is 28.8 °C higher than the ambient temperature, 45 + 28.8 = 73.8 °C.
- The radiant heat from the flame to the water cannon robot was calculated by assuming that the area from the oblique direction is the maximum. However, since vertical radiation is not applied to each irradiation surface (e.g., front, side, and top) of the water cannon robot, the radiation heat received from the actual flame on each surface is considered to be less than 20 kW/m^2. In contrast, the assumption mentioned above that the temperature of the backside of the radiation heat shielding cloth is 28.8 °C higher than the ambient temperature is based on the result of intermittent spraying of the experiment (e6) on the surface irradiated with 20 kW/m^2. This proves the safety of the robot.

Table 6 Design conditions for water cannon robots

Item	Value	Rationale for setting
Radiant heat intensity received by the robot	20 kW/m^2	The radiant heat for the largest oil tank fire, as assumed in "Radiant heat intensity in a petrochemical complex fire" section
Ambient temperature	45 °C	Assumed as the highest temperature under the scorching midsummer sun in Japan
Heat receiving and radiating area of the radiant heat-resistant exterior cover	3.71 m^2	Assuming irradiation from an oblique direction where the projected area of the robot is maximized [the robot's outline: (W) 1.4 m, (L) 2 m, (H) 1 m]
Internal heat generation of the robot	3.6 kW	Assume that 20% of the power consumed by the motor driver and 100% of the power consumed by others is dissipated as heat. The total internal heat generation of the actual water cannon robot is about 3.6 kW
Water cannon robot internal temperature target	60 °C or less	Select equipment that can withstand 60 °C as a design specification for the water cannon robot
Cross-section and length of radiant heat-resistant exterior fixing fitting	(W) 40 mm (H) 3 mm (L) 50 mm Qty 17 pcs	From the actual shape and number of fittings

- The water cannon robot housing temperature is equal to the temperature inside the robot (60 °C). The actual temperature of the housing is expected to be higher than the internal temperature, but assuming a lower temperature ensures that the robot is designed on the safe side for more cooling by natural convection.

These values substituted in Eq. (4) gives

$$RR_{\mathrm{SI}} = 367.30W \tag{21}$$

Calculation of RHT is also performed under similar assumptions as RR_{SI}.

- The backside temperature of the radiant heat shield fabric is 73.8 °C, which is 28.8 °C higher than the ambient temperature.
- The water cannon robot housing temperature is equal to the temperature inside the robot (60 °C).
- According to Table 6, the total area and length of the fixing brackets are as follows:

$$\begin{aligned} A &= \left\{\left(40\times10^{-3}\right)\times\left(3\times10^{-3}\right)\right\}\times17 \\ &= 2.04\times10^{-3}\mathrm{m}^2 \\ L &= 50\times10^{-3}\mathrm{m} \end{aligned}$$

These values substituted in Eq. (5) give

$$RHT = 9.18W \tag{22}$$

Calculation of H_{RI}

The internal heat generation of the electric components in the water cannon robot is 3.6 kW, as shown in Table 7.

R_{RO} is calculated under the following assumptions.

- The heat radiation from the water cannon robot to external air is in a windless condition, and the convective heat transfer coefficient K is 6.20 $\mathrm{W/m^2K}$, as estimated in the radiation heat-transfer experiment.

Table 7 Internal heat generation of installed equipment

Item	Internal heat generation [W]
Motor driver (drive system, hydraulic system)	3040.76
Camera, sensor, control system	263.4
Lighting, solenoid valves, solenoid brakes	297.8
Total	3601.96

- The radiation area of the water cannon robot comprises five surfaces, as described in Table 6, and is calculated as follows:

$$\{(1.4\times1)+(2\times1)\}\times2+(1.4\times2)=9.6\ \mathrm{m}^2$$

- The water cannon robot's housing temperature was assumed to equal the internal temperature (60 °C).
- These values substituted in Eq. (6) gives

$$R_{RO} = 892.8 \approx 893W \tag{23}$$

Considering that the environment reproduced by the two panel heaters in the radiation heat-transfer experiment has a radiant heat quantity that is approximately 11% lower than the targeted 20 $\mathrm{kW/m^2}$, it is considered that the backside of the radiant heat-shielding cloth will be higher than 28.8 °C. Therefore, the heat received by the robot was increased by 11% for use in the subsequent design calculation. In particular, it is assumed that RR_{SI} and RHT calculated using Eqs. (21) and (22) increase by 11%.

Therefore, the following adjusted values are applied in Eq. (3).

$$\begin{aligned} RR_{SI} &= 367.3\times1.11 = 407.7\ \mathrm{W} \\ RHT &= 9.18\times1.11 = 10.2\ \mathrm{W} \\ RR_{\mathrm{SI}} + RHT + H_{\mathrm{RI}} &= R_{\mathrm{RO}} + F_{\mathrm{RO}} \\ 407.7 + 10.2 + 3600 &= 893 + F_{\mathrm{RO}} \\ \therefore F_{\mathrm{RO}} &= 3124.9 \approx 3125\ \mathrm{W} \end{aligned} \tag{24}$$

Therefore, it is necessary to cool down the water cannon robot by ~3125 W by air displacement owing to the stack effect. The required airflow rate q to achieve this was calculated by substituting $\Delta\mathrm{T}=60$–45 °C into Eq. (7), as follows.

$$\begin{aligned} F_{\mathrm{RO}} &= C_{\mathrm{p}}\cdot\rho q\cdot T \\ 3125 &= C_{\mathrm{p}}\cdot\rho q\times(60-45) \\ \therefore q &= 0.1737 \approx 0.174\left[\frac{\mathrm{m}^3}{\mathrm{s}}\right] \end{aligned} \tag{25}$$

In contrast, the airflow rate of natural convection due to the stack effect was calculated using Eq. (8). The area A required for convection (here, the opening area of the upper surface required for the water cannon robot as an airflow path is shown.) is obtained by substituting the following values in Eq. (8)

$C=0.30$: the value estimated using Eq. (20). $h=1.3$ m: average height of the actual water cannon robot

aperture. $T_I = 60 + 273.15$ K: the internal temperature of the water cannon robot is 60 °C. $T_A = 45 + 273.15$ W K: ambient air temperature 45 °C.

$$0.174 = CA\sqrt{2gh\frac{T_I - T_A}{T_I}} \quad (26)$$
$$\therefore A = 0.541 \approx 0.54\ \mathrm{m}^2$$

Therefore, the top of the water cannon robot is designed to have an opening of 0.54 m^2.

Development of water cannon robot

To protect the water cannon robot from radiation heat by mounting the developed radiant heat-resistant exterior cover, an opening of 0.54 m^2 was required at the upper part of the robot; therefore, natural convection due to the stack effect could be expected. A vent (150 × 900 mm) provided on the upper part of the rear surface of the water cannon robot, is less than the required 0.54 m^2 opening. In addition, it is impossible to place a large opening in the front or the upper surface of the water cannon robot as it is exposed to the radiant heat from the flame.

The radiant heat-resistant exterior cover is a structure in which a plurality of parts are combined and mounted on a water cannon robot, with a gap of approximately 20–40 mm between each part for assembly reasons. Considering this gap as an opening, the total opening area, shown in red in Fig. 15, was reflected in the water cannon robot design to ensure an area of 0.54 m^2 or more.

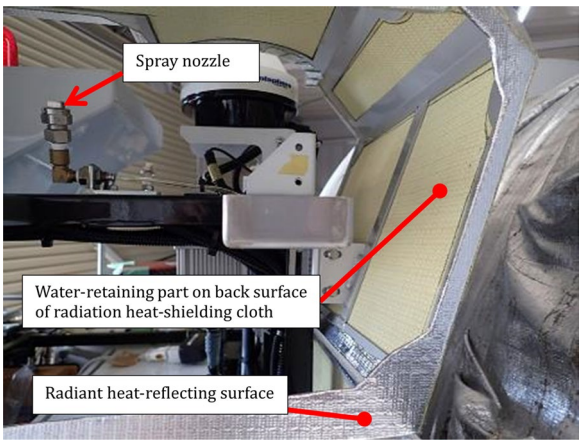

Fig. 16 Radiant heat-resistant exterior cover seen from inside the robot

- Dashed lines indicate gaps between the radiant heat-resistant exterior cover of 30 or 40 mm width.
- The robot had a 150 mm × 900 mm vent in the upper rear panel.
- The water cannon nozzle head (diameter 150 mm) was equipped with a 200 mm × 175 mm radiant heat-resistant exterior cover.

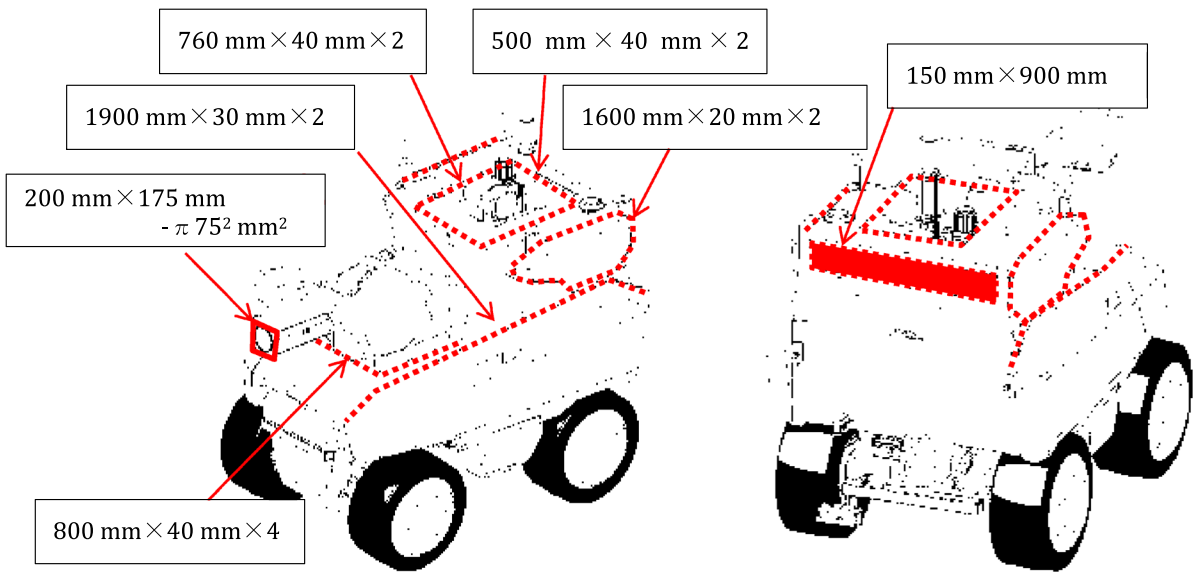

Fig. 15 Illustration of a water cannon robot opening

- The average opening height of the robot is 1.3 m, which was used in the calculation of Eq. (26).

The total area of the openings was calculated from Fig. 15 and 0.54 m^2 was secured.

$$\left\{\left(200\times175-\pi75^2\right)+(150\times900)+(((800\times4)+(500+760)\times2)\times40)+(1900\times2\times30)+(1600\times2\times20)\right\}\times10^{-6}=0.559\mathrm{m}^2>0.54\mathrm{m}^2$$

Figure 16 shows a photograph of the radiant heat-resistant exterior cover from the inside of the robot.

The cooling water tank used for spraying the cooling water, until external water was supplied, was calculated based on the experimental results. The spraying condition of the experiment (e6) in the radiation heat-transfer experiment was a 1/60 duty cycle (spray for 1 s, stop for 59 s) for 0.001 m^3/min water. The area of the radiant heat-resistant exterior cover was 0.04 m^2. Therefore, the amount of spray water per 1.0 m^2 is calculated as follows.

$$0.001\left[\mathrm{m}^3/\mathrm{min}\right]\times\frac{1}{60}\times\frac{1}{0.04\left[\mathrm{m}^2\right]}=4.17\times10^{-4}\left[\mathrm{m}^3/\left(\mathrm{min}\ \mathrm{m}^2\right)\right] \quad (27)$$

The amount of spray water required for the robot was calculated using the area ratio of the radiant heat-resistant exterior cover. The front, both sides, and top surfaces of a robot heading for a fire scene are likely to receive radiation heat from the flames, and the total area of these surfaces is calculated from Table 6 as $(1.4\times1)+(2\times1)+(1.4\times2)=6.2$ m^2. The amount of spray water required is then calculated using Eq. (27), as follows.

$$4.17\times10^{-4}\times6.2=2.59\times10^{-3}\mathrm{m}^3/\mathrm{min} \quad (28)$$

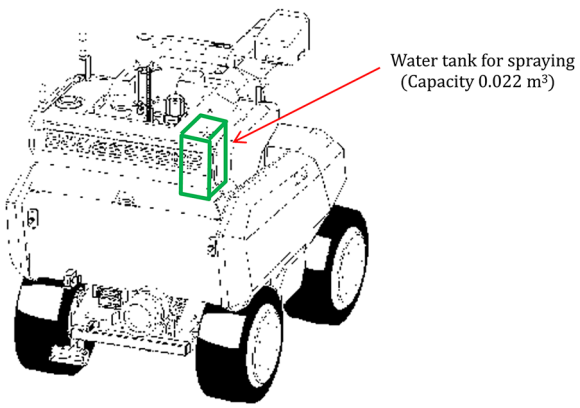

Fig. 17 Position diagram of the water tank

This is approximately 1/80th of the amount of water required by the conventional self-protection sprinkling mechanism, which requires 0.2 m^3/min.

During the operation of the water cannon robot, the period of use of water in the cooling water tank, that is, the time from when the water cannon robot enters a high radiant heat environment near the flame to when external water for fire extinguishing is supplied was set to 450 s as shown in Table 8, assuming an actual fire-operation scenario.

The amount of water required for spraying on the radiant heat-resistant exterior cover, until the water for extinguishing the fire is supplied, is then calculated as:

$$2.59\times10^{-3}\mathrm{m}^3/\mathrm{min}\times\frac{450\ \mathrm{s}}{60\mathrm{s}/\mathrm{min}}=0.01943\ \mathrm{m}^3 \quad (29)$$

Table 8 Time estimation table for water cannon robot requiring cooling spray

Operation	Required time (s)	Notes
Move to water discharge position	40	The robot, traveling at 1.5 m/s, is expected to move 50 m to the water-discharge position in the vicinity of the flame where radiant heat is strong
Water supply hose laying work	250	This involves laying out hose (of max. 300 m length) from the discharge location to the water source. The required time was set from the actual work scenario
Water supply hose connection and water supply	160	The required time was set from the actual work scenario
Total	450	

Thus, the mountable 0.022 m^3 water tank, shown in Fig. 17, has approximately 13% more capacity than what is required.

Discussion

To protect a water cannon robot working at a fire scene from the flame's radiation heat, the cooling method that reflects most of the heat was proposed. The radiation heat-transfer experiment using a simplified robot model identified the relationship between the air displacement by natural convection of the stack effect and temperature rise in the simplified model owing to the spray pattern (spray duty cycle) of cooling water, and the validity of the basic concept was confirmed. The water cannon robot was designed using the estimated K and C parameters, with an opening for natural convection and a water tank mounted to supply the cooling water. The designed water cannon robot satisfied the requirements of heat projection. Therefore, it can play an active role in a fire scene under 20 kW/m^2 radiation heat.

In the experiment, the radiant heat radiated from the heat source to the simplified model was 11% lower than the target value of 20 kW/m^2. This does not affect the estimation of K and C parameters related to the heat balance. However, in the design of the water cannon robot, because the heat input to the robot is calculated using the temperature of the experimental result, the calculations were made considering this difference to ensure thermal design safety.

The maximum heat reaching the robot surface is considered to be radiated from the right (or left) diagonal upward direction. Therefore, the maximum area of the orthographic projection with a cuboid robot is regarded as the heat-receiving surface. However, in this case, the radiation to each surface (e.g., front, side, top) of the robot is not vertical, so the radiation heat received from the flame will be less than 20 kW/m^2. When cooling using the same water spray pattern as in the radiation heat-transfer experiment, it can be assumed that the backside temperature of the radiant heat-shielding cloth becomes lower than that of the experimental result. This implies that the temperature will be lower than "ambient temperature + 28.8 °C". Therefore, it is considered that the design has been made in consideration of safety.

If we need to further improve the cooling effect of the robot, measures such as changing the air substitution by natural convection of the stack effect to forced convection equipped with a fan, increasing the opening area of the upper part, or increasing the amount of mist spray water are considered. This requires redesigning the robot, for example, by increasing the battery capacity and reviewing the structure and arrangement of the robot. However, the proposed radiant heat-resistant exterior cover makes it possible to realize a smaller and lighter robot than conventional robots that require a large amount of water. However, the radiant heat of 20 kW/m^2, which is a considerably high amount of radiation, such as in petroleum complex fires, can be reproduced only in a square area of at most 200 mm even if a high-power panel heater is used, as in our experiment in Fig. 9. Therefore, the effectiveness of the proposed radiant heat-resistant exterior cover can only be confirmed when operated in an industrial complex fire.

Conclusion

In environments where flames generate intense radiant heat, such as petroleum complex fires, a robot that can engage in firefighting activities, such as fire extinguishing and cooling, is required. This study proposes a radiant heat-resistant exterior cover attachable to a robot that requires only 1/80th volume of water compared to the conventional self-sprinkling method.

A radiation heat-transfer experiment with a simplified robot model determined the design parameters of the radiant heat-resistant exterior cover. A 0.022 m^3 water tank mounted on the interior frame of the firefighting robot was found sufficient to protect a water cannon robot with a width of 1.4 m, a mass of 2000 kg, and a water discharge capacity of 4 m^3/min in a radiant heat environment of 20 kW/m^2 for more than 7.5 min, which is considered sufficient before additional water can be supplied from the outside.

The reflection of radiation with vaporization and natural convection concept is applicable to protect the firefighting robots.

The proposed method will contribute to the miniaturization and weight reduction of existing robots equipped with large water tanks for self-protection sprinkling. The water cannon robot equipped with the proposed radiant heat-resistant exterior cover was deployed to the Ichihara Fire Department in JAPAN, which has jurisdiction over a petrochemical complex that handles crude oil, naphtha, ethylene, and other fuels.

Acknowledgements

This research is a part of "Research and development of firefighting robots for energy and work infrastructure disaster response" (2014–2020 fiscal yare) from the Ministry of Internal Affairs and Communications JAPAN.

Author contributions

JF planned and designed the research experiments and wrote the paper. JF and YT conducted the experiments and organized the data. HA contributed to the planning of the heat evaluation method. KO and ST contributed to data interpretation and the drafts and gave final approval for publication. All authors read and approved the final manuscript.

Funding

Not applicable.

Availability of data and materials
Not applicable.

Declarations

Competing interests
The authors declare that they have no competing interests.

Author details
[1]Mitsubishi Heavy Industries, LTD, 1-1, Wadasaki-cho 1-chome, Hyogo-ku, Kobe, Hyogo 652-8585, Japan. [2]Department of Precision Engineering, The University of Tokyo, Tokyo, Japan. [3]National Research Institute of Fire and Disaster, Tokyo, Japan. [4]NICHe, Tohoku University/RIKEN AIP, Sendai, Japan. [5]GSIS, Tohoku University, Sendai, Japan.

Received: 30 January 2022 Accepted: 10 May 2022
Published online: 26 May 2022

References

1. Director of Hazardous Materials Control Division (1980) Fire Defense Agency, fire hazard no. 80, July 1, 1980 (**Japanese title translated in English**)
2. Moshashaei P, Alizadeh SS, Khazini L, Asghari-Jafarabadi M (2017) Investigate the causes of fires and explosions at external floating roof tanks: a comprehensive literature review. J Fail Anal Prev 17:1044–1052
3. Extraordinary Disaster Management Office, Fire and Disaster Management Agency (2013) Guidelines for disaster prevention assessment of petroleum complexes, March 2013 (**Japanese title translated in English**)
4. Nishi H (2004) Tank fire in Tomakomai City, Hokkaido. Jpn Soc Saf Eng 43:54–55 (**Japanese title translated into English**)
5. Fire of a floating roof tank of crude oil caused due to a large earthquake and full face fire of another floating roof tank two days later. http://www.shippai.org/fkd/en/cfen/CC1300013.html. Accessed 30 Mar 2022
6. Cosmo Oil Co., Ltd. (2011) Fire and explosion at the Chiba refinery. https://ceh.cosmo-oil.co.jp/csr/publish/sustain/pdf/2011/sus2011_2.pdf. Accessed 30 Mar 2022 (**Japanese title translated into English**)
7. Cosmo Oil Co., Ltd. Chiba Refinery (2012) Disaster prevention activities for LPG tank fire and explosion accidents during the Great East Japan Earthquake. Hazard Mater Saf Techn Assoc Saf Tomorrow 143:27–38
8. Nippon Shokubai Co., Ltd. (2013) An accident investigation board. Nippon Shokubai Himeji plant acrylic acid plant explosion and fire investigation report. (**Japanese title translated into English**)
9. Fujita J, Amano H, Ohno K, Tadokoro S (2020) Development of firefighting robot system applicable to petroleum complex fires. In: Proceedings of the 2020 JSME conference on robotics and mechatronics in Kanazawa. 2A1-A02
10. Unmanned firefighting robotic vehicle "Sentry". https://www.popularmechanics.com/science/environment/a25051641/mythbuster-jamiehynemman-wildfire-tank-sentry/. Accessed 30 Mar 2022
11. https://www.rac-germany.com/products/oilfield_trucks/fire_fighting_vehicle.html. Accessed 30 Mar 2022
12. Wei tech explosion-proof fire fighting robot. https://universalfireprotection.com.pk/weistech-explosion-proof-fire-fighting-robot/. Accessed 30 Mar 2022
13. Tsukiyama T (1988) The present status of R&D in the advanced robot technology project. J Soc Instrum Control Eng. 27:497–500. https://www.jstage.jst.go.jp/article/sicejl1962/27/6/27_6_497/_pdf/-char/ja. Accessed 30 Mar 2022. (**Japanese title translated in English**)
14. Özge TOK, Keçeci EF (2008) Design and manufacturing of a fireproof fire rescue robot. Izmire Institute of Technology, pp 36–37. https://gcris.iyte.edu.tr/bitstream/11147/3938/1/T000732.pdf. Accessed 30 Mar 2022

Publisher's Note